THE JOURNAL OF BIOLOGICAL CHEMISTRY VOL. 285, NO. 23, pp. 17713–17724, June 4, 2010

Characterization of the Chemokine CXCL11-Heparin Interaction Suggests Two Different Affinities for Glycosaminoglycans*[S]

Received for publication, November 6, 2009, and in revised form, February 26, 2010 Published, JBC Papers in Press, April 2, 2010, DOI 10.1074/jbc.M109.082552

India C. Severin[‡1], Jean-Philippe Gaudry[‡1], Zoë Johnson[‡], Andreas Kungl[§], Ariane Jansma[¶], Bernd Gesslbauer[§], Barbara Mulloy[‖], Christine Power[‡], Amanda E. I. Proudfoot[‡2], and Tracy Handel[¶]

From the [‡]Merck Serono Geneva Research Centre, 9 Chemin des Mines, 1202 Geneva, Switzerland, [§]ProtAffin Biotechnologie AG, A-8020 Graz, Austria, the [‖]National Institute for Biological Standards and Control, Blanche Lane, South Mimms, Potters Bar, Hertfordshire EN6 3QG, United Kingdom, and the [¶]Skaggs School of Pharmacy and Pharmaceutical Science, University of California, San Diego, La Jolla, California 92093-0684

Chemokines orchestrate the migration of leukocytes in the context of homeostasis and inflammation. In addition to interactions of chemokines with receptors on migrating cells, these processes require interactions of chemokines with glycosaminoglycans (GAGs) for cell surface localization. Most chemokines are basic proteins with Arg/Lys/His residue clusters functioning as recognition epitopes for GAGs. In this study we characterized the GAG-binding epitopes of the chemokine I-TAC/CXCL11. Four separate clusters of basic residues were mutated to alanine and tested for their ability to bind to GAGs *in vitro* and to activate the receptor, CXCR3. Mutation of a set of basic residues in the C-terminal helix (the 50s cluster, ^{57}KSKQAR^{62}) along with Lys^{17}, significantly impaired heparin binding *in vitro*, identifying these residues as components of the dominant epitope. However, this GAG mutant retained nearly wild type receptor binding affinity, and its ability to induce cell migration *in vitro* was only mildly perturbed. Nevertheless, the mutant was unable to induce cell migration *in vivo*, establishing a requirement of CXCL11 for GAG binding for *in vivo* function. These studies also led to some interesting findings. First, CXCL11 exhibits conformational heterogeneity, as evidenced by the doubling of peaks in its HSQC spectra. Second, it exhibits more than one affinity state for both heparin and CXCR3, which may be related to its structural plasticity. Finally, although the binding affinities of chemokines for GAGs are typically weaker than interactions with receptors, the high affinity GAG binding state of CXCL11 is comparable with typical receptor binding affinities, suggesting some unique properties of this chemokine.

Chemokines belong to a family of small chemotactic cytokines that selectively recruit and activate specific leukocytes during inflammation and routine immunosurveillance (1, 2). The chemokines of all four subclasses (CC, CXC, CX3C, and C) have a remarkably conserved three-dimensional tertiary structure, but many form dimers, tetramers, and higher order oligomers, and although monomeric forms are sufficient for cell migration *in vitro* (3–5), for some chemokines, oligomerization is required for function *in vivo* (6, 7). All chemokines exert their biological activity by binding to seven-transmembrane G protein-coupled receptors, which are also subdivided into four classes analogous to the ligand classification (8). Additionally, many chemokines interact with the glycosaminoglycan (GAG)[3] moieties of proteoglycans on endothelial cells and the extracellular matrix (6). GAGs enable the surface immobilization of chemokines, thereby creating haptotactic gradients in order to direct leukocytes to sites of inflammation (9). As demonstrated with a series of chemokine mutants that were impaired in their ability to bind GAGs, when the GAG interaction is disrupted, chemokines lose the ability to efficiently recruit cells *in vivo*, even when chemotaxis *in vitro* is unperturbed (7).

GAGs are negatively charged linear polysaccharides that have an exceptional range of size and sequence variability, including patterns of sulfation and acetylation. All chemokines interact with heparin, which serves as a model compound for heparan sulfate, the most ubiquitous class of GAG that is expressed on virtually every cell in the body. Beyond their role in localizing chemokines, the interaction with GAGs may contribute to the selectivity and fine tuning of the chemokine system, which appears promiscuous and redundant when one only considers the pairing of ligands and receptors. For example, as cells can change their carbohydrate composition in pathological situations, such as inflammation and cancer (10–13), interactions with GAGs may play an important role in disease progression by accumulating specific chemokines that recruit specific leukocyte populations (6, 14).

GAG binding sites have been delineated for several chemokines and, when mapped onto their surfaces, show considerable topological diversity (15–22). A BB*X*B motif (where B repre-

* This work was supported, in whole or in part, by National Institutes of Health Grant RO1-AI37113 (T. M. H.). This work was also supported by the Lymphoma Research Foundation, United States Department of Defense Grant USAMRAA W81XWH0710446, and European Union FP6 INNOCHEM Award LSHB-CT-2005-518167 (to A. E. I. P.).

[S] The on-line version of this article (available at http://www.jbc.org) contains supplemental Figs. 1–3.

[1] Both authors contributed equally to this work.

[2] To whom correspondence should be addressed. Tel.: 41-22-414-98-00; Fax: 41-22-414-97-71; E-mail: amanda.proudfoot@merckserono.net.

[3] The abbreviations used are: GAG, glycosaminoglycan; HSQC, heteronuclear single quantum coherence; RANTES, regulated upon activation, normal T-cell expressed and secreted; IFN, interferon; SAB, standard assay buffer; SPA, scintillation proximity assay; WT, wild type; HPLC, high pressure liquid chromatography; CHO, Chinese hamster ovary; PBS, phosphate-buffered saline.

sents a basic residue) has been shown to be responsible for GAG binding in the 40s loop for MIP-1α (macrophage inflammatory protein-1α)/CCL3, MIP-1β/CCL4, and RANTES/CCL5 whereas SDF-1 (stromal cell-derived factor-1)/CXCL12 mediates GAG binding through a BB*X*B motif in the 20s loop. MCP-1 (monocyte chemotactic protein 1)/CCL2 similarly utilizes the 20s loop (residues Arg^{18}, Lys^{19}, Lys^{49}, and Arg^{24}) as its principal GAG binding site but also has contributions from His^{66} and Lys^{58} in the C-terminal helix, similar to the involvement of the helix in interleukin-8/CXCL8 (Lys^{20} and Arg^{68}).

In a survey of the relative affinity of chemokines for heparin, we noted that I-TAC (IFN-γ-inducible T-cell α-chemoattractant)/CXCL11 binds to heparin-Sepharose more tightly than most chemokines with the exception of CCL5 (6) and were therefore interested in examining the GAG binding epitopes on this chemokine. CXCL11 was first discovered in astrocytes through cDNA sequencing (23) and was subsequently shown to be induced by IFN-γ in a wide variety of additional cells, including bronchial epithelial cells, basal keratinocytes, neutrophils, and endothelial cells (24–26). CXCL11 signals through a single receptor, CXCR3, which it shares with two additional chemokines, IP-10 (IFN-γ-inducible 10-kDa protein)/CXCL10 and MIG (IFN-γ-induced monokine)/CXCL9. CXCR3 is expressed on activated T-lymphocytes, mainly of the Th1 subtype, as well as on a subset of B-cells, monocytes, and NK cells (27). Although these three chemokines are agonists of CXCR3, they have all been described as natural antagonists of CCR3 in Th2-type responses (28). Furthermore, CXCL11 was recently shown to bind to a second receptor, CXCR7, but it does not elicit classic signaling responses, such as calcium flux or cell migration (29).

To define the GAG binding epitopes of CXCL11, we first mutated four clusters of basic residues to alanine: a BB*X*B motif located in the N-terminal region (^{5}KRGR^{8}) and three clusters located in the 40s loop (^{46}KENKGQR^{52}), in the 50s loop (^{57}KSKQAR^{62}), and in the 60s loop toward the C terminus (^{66}KKVERK^{71}). *In silico* investigation by modeling with an 11-mer oligosaccharide, also suggested the involvement of Lys^{17}, which was combined with the 50s mutations due to its spatial proximity. Several methods have been used to define GAG binding sites, but they do not always give consistent results, and typically multiple methods are best used in concert for the most definitive answers (30–32). We therefore analyzed the CXCL11 mutants by affinity chromatography on heparin-Sepharose, saturation binding assays on immobilized heparin, mass spectrometry identification of a protected fragment from a tryptic digestion of a heparin-CXCL11 complex, and last, the ability to recruit cells *in vitro* and *in vivo*. Consensus data from both the *in vitro* and *in vivo* experiments suggest that the major epitope for GAG binding consists of a relatively diffuse site, including the 50s loop and Lys^{17}. The classical BB*X*B heparin binding motif in the N-terminal region did not contribute to GAG binding but was shown to be involved in receptor binding, together with a contribution from the 40s loop. Last, analysis of these mutants in an equilibrium competition binding assay on solid-phase heparin with soluble heparin as competitor identified an unusually high affinity (picomolar) binding site for CXCL11, which was subsequently found to also exist for CCL5 but not for CCL2 or CXCL12. Future studies will address whether this high affinity binding site is present in other GAG families/chemokines as well as the structural nature and biological relevance of the interactions.

EXPERIMENTAL PROCEDURES

Reagents—Unless stated otherwise, all chemicals were purchased from Sigma. Commercial CXCL11 was obtained from PeproTech. The heparin used in the assays was unfractionated heparin sodium salt supplied by Sigma (5–30 kDa; catalogue no. H3393) or low molecular weight heparin sodium salt (3 kDa; catalogue no. H3400). Enzymes were purchased from New England Biolabs, and chromatographic material was from GE Healthcare. EC_{50} and IC_{50} values were calculated using GraphPad Prism software, employing the equation, sigmoidal dose response (variable slope), with Y = bottom + (top − bottom)/(1 + 10^((log EC_{50} − X)*Hill slope), where X is the logarithm of concentration and Y is the response. For the double binding site curves, GraphPad Prism software was used, employing the equation for a biphasic dose response.

Molecular Modeling—Docking calculations for heparin oligosaccharides with the NMR structure of CXCL11 (Protein Data Bank code 1RJT) were carried out using a validated protocol for the identification of heparin binding sites on protein surfaces (33). This program allows limited flexibility in the ligand structure but keeps the protein rigid. Three oligosaccharide structures were investigated, all taken from the NMR structure of heparin (Protein Data Bank code 1HPN). Two structures were pentasaccharide substructures, with iduronate residues in the $^{1}C_{4}$ and $^{2}S_{0}$ conformations, respectively. All exocyclic bonds other than the glycosidic linkages were allowed to rotate. The third oligosaccharide was the full endecasaccharide, which was maintained in a rigid conformation with no rotatable bonds. The Protein Data Bank entry for CXCL11 contains coordinates for 10 structures compatible with the NMR data, which vary primarily in the flexible N-terminal region (34). All three oligosaccharides were docked with the first of the 10 structures, whereas the endecasaccharide was docked with all 10 structures in the ensemble. Docking was performed as described (33), using the program Autodock version 2.4. Specifically, an 84-Å cubical grid, with a grid spacing of 0.7 Å centered on the mean of the protein coordinates, was used so that the entire protein surface was available to the ligand. For the docking procedure, 128 simulated annealing runs of 300 cycles were performed. No clustering was carried out because no analysis of binding modes was required.

Generation of CXCL11 Mutants—Mutagenesis was performed by PCR. The mutants were created in one or two PCR steps, depending on the relative position of the mutations. A pET24d plasmid with the CXCL11 sequence was used as the template; in addition to the WT sequence, it contains the mutation F73W, which was introduced for protein quantification, and an N-terminal tag (MKKKWP) followed by a caspase 8 cleavage site (LETD) to produce the native N terminus. The mutations K17A and K38A were made in the context of the 50s loop mutant using the QuikChange mutagenesis kit (Stratagene).

Protein Purification and Characterization—The mutant plasmids were transformed into competent BL21 Star *Escherichia coli* cells. 5 liters of LB medium containing kanamycin were inoculated and, after induction with 1 mM isopropyl-β-D-thiogalactopyranoside at $A_{600} = 0.6$, allowed to grow for 3.5 h at 37 °C before harvesting. The cells were resuspended in lysis buffer (50 mM Tris/HCl buffer, pH 8, containing 10 mM $MgCl_2$, 5 mM benzamidine/HCl, 1 mM dithiothreitol, 0.1 mM phenylmethylsulfonyl fluoride, and 20 mg/liter DNase). Cells were broken by three passages through a French press. The suspension was then centrifuged at 10,000 × *g* for 60 min at 4 °C. The inclusion body pellet containing the recombinant protein was solubilized at 1 g/20 ml in 0.1 M Tris/HCl, pH 8.0, containing 6 M guanidine/HCl and 1 mM dithiothreitol and stirred for 30 min at 60 °C. The proteins were renatured by dropwise 10-fold dilution into 0.1 M Tris/HCl buffer, pH 8.0, containing 0.01 mM oxidized glutathione and 0.1 mM reduced glutathione, with stirring overnight at 4 °C. The pH was adjusted to 4.5 with acetic acid, and the conductivity was lowered below 20 millisiemens by dilution with distilled H_2O. The solution was applied to an SP Sepharose column (16/10) previously equilibrated in 50 mM sodium acetate, pH 4.5. Protein was eluted with a 0–2 M gradient of NaCl in the same buffer. Fractions containing CXCL11 or mutant were pooled and dialyzed twice against 1% acetic acid and finally against 0.1% trifluoroacetic acid. Insoluble material was removed by centrifugation at 10,000 × *g* for 30 min, and the supernatant was lyophilized.

In order to remove the leader tag sequence, the lyophilized proteins were dissolved at 1 mg/ml in H_2O and applied to PD-10 columns previously equilibrated with caspase 8 cleavage buffer (25 mM Tris, pH 7.5, containing 15% glycerol, 150 mM NaCl, and 2 mM EDTA). The MKKKWPLETD leader sequence was cleaved by incubation with caspase 8 (enzyme/substrate, 1:10, w/w) for 30 min at 37 °C. The cleaved proteins were separated from uncleaved protein by reverse phase HPLC (Alliance HPLC, Waters; column: EC 250/4 Nucleosil 300-7 C8, Macherey-Nagel) using a linear gradient of 25–50% acetonitrile in 0.1% trifluoroacetic acid over 20 min at a flow rate of 2 ml/min. Protein sequences were verified by matrix-assisted laser desorption ionization mass spectrometry, which confirmed the formation of the two disulfide bonds. The function of the WT protein was confirmed by receptor binding and chemotaxis assays as described below.

Proteolytic Footprinting—For GAG footprinting experiments, CXCL11 was proteolytically digested with trypsin in the presence and in the absence of heparin. For this purpose, CXCL11 (20 pmol) was incubated for 1 h at 20 °C with a 10-fold molar excess of heparin in 50 mM NH_4HCO_3, pH 8.0, containing 150 mM NaCl to suppress nonspecific interactions. After the addition of trypsin (sequencing grade unmodified, Roche Applied Science) in an enzyme/substrate ratio of 1:10 (w/w), proteolytic cleavage was carried out at 37 °C for 18 h. The digest was stopped by adjusting the pH to 2.5 with formic acid. The resulting peptide fragments were identified by nano-HPLC-tandem mass spectrometry as described previously (35). Potential GAG binding epitopes on the chemokine were identified as non-digested (protected) peptides observed in the presence of heparin but missing in the absence of heparin.

Heparin-Sepharose and S-Sepharose (Cation Exchange) Chromatography—As an initial screen to identify residues comprising the GAG-binding epitope, the amount of salt required to elute WT and mutant CXCL11 from a heparin-Sepharose column was determined. 100 μg of either CXCL11 or mutant protein was loaded onto a heparin-Sepharose column (5/5), equilibrated in 50 mM Tris/HCl, pH 7.5, and eluted with a linear gradient of 0–2 M NaCl in the same buffer, as described previously (21). To measure the contribution of various residues to the specificity of the interaction, the amount of salt required to elute mutants from a nonspecific S-Sepharose column (SP column 5/5) was also determined using the same protocol and compared with the elution from the heparin-Sepharose column. The specificity index is related to ΔΔNaCl as calculated from the formula below, where the superscripts *Hep* and *S* refer to elution from the heparin-Sepharose or S-Sepharose column, respectively (19),

$$\Delta\Delta[\mathrm{NaCl}] = \Delta[\mathrm{NaCl}]^{Hep} - \Delta[\mathrm{NaCl}]^{S} \quad \text{(Eq. 1)}$$

where $\Delta[\mathrm{NaCl}]^{Hep} = [\mathrm{NaCl}]^{Hep}$ WT $- >$ $[\mathrm{NaCl}]^{Hep}$ mutant, and $\Delta[\mathrm{NaCl}]^{S} = [\mathrm{NaCl}]^{S}$ WT $- [\mathrm{NaCl}]^{S}$ mutant.

Saturation Binding Assay to Immobilized Heparin—In order to test the ability of WT CXCL11 and the mutants to bind to heparin, a colorimetric enzyme-linked immunosorbent assay on the surface of microtiter plates was used (Epranex Plates, Plasso Technology Ltd., Sheffield, UK). The plate was coated with heparin by incubation with a heparin solution (25 μg/ml) in PBS (200 μl/well) overnight at room temperature and in the absence of light, as described by the supplier. The liquid was discarded, and the plate was washed three times with standard assay buffer (SAB) (100 mM NaCl, 50 mM NaOAc, 0.2% (v/v) Tween 20, pH 7.2). 250 μl of blocking solution (0.2% (w/v) gelatin in SAB) was then added per well, and the plate was incubated for 1 h, protected from light. Dilution series ranging from 10^{-6} to 10^{-12} M CXCL11 and mutant proteins were prepared. 100-μl samples were then transferred in duplicate to the heparin-coated Epranex plate and incubated for 2 h at room temperature with gentle shaking. The wells were washed three times with SAB. For detection, a biotinylated anti-human CXCL11 antibody (R&D Systems; dilution 1:500 in SAB) was used. 200 μl of antibody solution was added to each well and incubated for 1 h at room temperature. The plate was then washed three times with SAB and incubated with ExtrAvidin-AP (Sigma) in blocking solution (1:10,000). After three washes with SAB, 200 μl of the development reagent (*p*-nitrophenyl phosphate liquid substrate system, Sigma) was added to each well. The plate was incubated for 40 min at room temperature, and the absorbance was measured at 405 nm.

Immobilized Heparin Competition Binding Assay—Competition experiments were performed in 96- or 384-well filter plates (Millipore MultiScreen, 0.22-μm pore size, low protein binding) in a total volume of 100 or 40 μl/well, respectively. Each well contained 0.1 nM [^{125}I]chemokine, heparin-Sepharose beads, or binding buffer as a background control and 0–2 mg/ml heparin. This corresponds to 0–667 μM for the fractionated low molecular mass 3-kDa heparin, H3400. Using an average molecular mass of 17.5 kDa for unfractionated heparin,

H3393, which consists of chains ranging from 5 to 30 kDa, the corresponding concentration range is 0 to ~115 μM. The mass of heparin on the beads corresponded to 0.125 or 0.05 μg/well for 96- or 384-well plates, respectively. The plates were incubated by shaking at room temperature for 4 h in binding buffer (50 mM Tris, pH 7.4, containing 0.5% bovine serum albumin, 5 mM $MgCl_2$, and 1 mM $CaCl_2$). The beads were washed three times with 200 μl of binding buffer containing 0.15 M NaCl by vacuum filtration. For CCL5, it was necessary to add 0.15 M NaCl to the binding buffer during the incubation and 0.5 M NaCl to the binding buffer for the washes to avoid nonspecific binding to the filter plate. The filters were air-dried, 30 μl of scintillation fluid was added to each well, and the radioactivity was measured in a Wallac Microbeta counter. Each experiment was performed in triplicate.

Equilibrium Competition Receptor Binding Assays—The assays were carried out on membranes from CHO transfectants expressing CXCR3, using a scintillation proximity assay (SPA) with [^{125}I]CXCL11 as the tracer. Serial dilutions of the unlabeled chemokines, covering the range indicated in the figure, were prepared in binding buffer (50 mM Tris/HCl, pH 7.2, containing 1 mM $CaCl_2$, 5 mM $MgCl_2$, and 0.5% bovine serum albumin). Wheat germ SPA beads (Amersham Biosciences) were solubilized in PBS at 50 mg/ml and diluted in binding buffer to a concentration of 10 mg/ml, and membranes of CHO transfectants expressing CXCR3 were solubilized at 20 μg/ml in binding buffer. Equal volumes of membrane and SPA bead solutions were mixed before adding them to the assay. The final membrane concentration in the assay was 5 μg/ml, and the concentration of [^{125}I]CXCL11 was 0.05 nM. The plates (Corning, 96-well, flat and clear bottom) were incubated at room temperature under agitation for 4 h. Radioactivity was counted with a Microbeta counter for 1 min/well.

Chemotaxis Assays—Chemotaxis assays were carried out in 96-well microplates (Neuro Probe ChemoTx) with L1.2/CXCR3 cell transfectants. The cells were cultured in RPMI 1640 medium containing 5% inactivated fetal calf serum, L-glutamine (2 mM), 25 mM HEPES, 0.05 mM β-mercaptoethanol, and 0.8 mg/ml Geneticin G-418. The day before the assay, *n*-butyric acid (5 mM) was added to the culture medium. The cells were collected by centrifugation (600 × *g*) and resuspended at a concentration of 0.85 × 10^6/ml in RPMI 1640 medium containing 5% heat-inactivated fetal calf serum without phenol red. A dilution series of CXCL11 and mutants was prepared covering the range of 10^{-6} to 10^{-12} M in RPMI medium without phenol red, and 30 μl were placed in the wells of the lower plate. A filter membrane (8-μm pore size) was placed over the plate. 25 μl of the cell solution (2.5 × 10^4 cells) was deposited on top of the membrane of each well. The chamber was incubated for 5 h at 37 °C under 5% CO_2. The cell suspension was then washed with PBS, and the filter was removed. The migrated cells in the lower wells were transferred to a black plate using a 96-well funnel adaptor and frozen for at least 2 h at −80 °C. The plate was thawed, and a solution of CyQUANT dye/cell-lysis buffer mix (Molecular Probes, 200 μl) was added to each well. The fluorescence was measured using a Victor^2 Wallac plate reader.

Peritoneal Cellular Recruitment—Because CXCR3 is expressed on activated Th1 cells, mice were sensitized to activate T cells prior to the peritoneal recruitment assay. On day 0, 8–12-week-old female Balb/c mice were sensitized by five subcutaneous injections (4 × 50 μl into each limb and 1 × 100 μl into the scruff of the neck) of 10 nM CpG-ODN (Microsynth) mixed with 100 μg of ovalbumin (Sigma, Grade V) in sterile PBS. Cellular recruitment was induced on day 6 by intraperitoneal injection of 10 μg of CXCL11 or mutant diluted in 0.2 ml of sterile, LPS-free NaCl (0.9%). Mice were sacrificed with aerosolized CO_2 4 h later. Peritoneal lavage was performed with 3 × 5 ml of PBS, and the lavages were pooled. Cells were centrifuged at 1500 rpm for 5 min and resuspended in 1 ml of PBS, and total leukocytes were counted with a hemacytometer.

NMR Spectroscopy—^{15}N-Labeled CXCL11 was made by bacterial expression in minimal media as described previously (36). All spectra were run on Bruker Avance II 600-MHz spectrometer with a TCI CryoProbe. ^{1}H-^{15}N HSQC spectra were recorded under several conditions of pH and temperature and were screened for spectral quality, but the protein consistently showed conformational heterogeneity. For the representative spectra shown in Fig. 7, the sample was prepared at a concentration of 1 mM in 10 mM acetate buffer, pH 5.3, and the data were collected at 23 °C. For the pulsed field gradient diffusion measurements, the ^{15}N-labeled CXCL11 sample was prepared in 50 mM acetate-d_6, pH 5.6, and the experiments were conducted using the pulse sequence ledbpgpprwg2s with the Bruker macro DOSY. Values for the diffusion time, d20 (Δ) and the gradient pulse length, p30 (δ*0.5) were 150 and 2.0 ms, respectively. The self-diffusion coefficients (D_s) were calculated using the Bruker program T_1/T_2 relaxation with manual integration for peaks at 7.0, 3.0, 2.0, and 0.7 ppm for each proton spectrum. The resulting decay curves were fit, and the D_s values were calculated using the equation,

$$I(g) = I(0)\exp(-(\gamma g\delta)^2 D(\Delta - (\delta/3))) \qquad \text{(Eq. 2)}$$

where $I(0)$ is 4.167 × 10^{-1}, γ is 4.258 × 10^3 Hz/G, g was calibrated at 5.784 gauss/mm, δ was set to 4.0 ms, and Δ was set to 150 ms. The theoretical change in D_s from a monomeric to dimeric form of a protein may be estimated by approximating the monomer-monomer interaction as a hard sphere molecular contact. Using the expected change in the frictional coefficient in conjunction with the Stokes-Einstein equation, the theoretical ratio $D_{s,\mathrm{dimer}}/D_{s,\mathrm{monomer}}$ is 0.75 (37). Each sample was run in triplicate, and the D_s values were averaged over the three experiments.

RESULTS

Because the primary GAG binding sites of many chemokines have been frequently localized to residues close in sequence, such as BB*X*B and BB*XX*B motifs, we initiated our characterization of the GAG site on CXCL11 by individually mutating four clusters of basic residues. Within each cluster, Lys and Arg residues were replaced by Ala because they are frequently found to be the dominant amino acids involved in heparin binding. The mutants are referred to as the 10s (^{5}AAGA^8), the 40s (^{46}AENAGQA^{52}), the 50s (^{57}ASAQAA^{62}), and the 60s

A

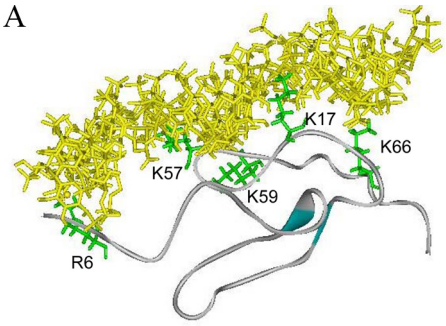

B

```
          10        20        30        40        50        60        70
WT   FPMFKRGRCL CIGPGVKAVK VADIEKASIM YPSNNCDKIE VIITLKENKG QRCLNPKSKQ ARLIIKKVER KNF
10s  FPMFAAGACL CIGPGVKAVK VADIEKASIM YPSNNCDKIE VIITLKENKG QRCLNPKSKQ ARLIIKKVER KNF
40s  FPMFKRGRCL CIGPGVKAVK VADIEKASIM YPSNNCDKIE VIITLAENAG QACLNPKSKQ ARLIIKKVER KNF
50s  FPMFKRGRCL CIGPGVKAVK VADIEKASIM YPSNNCDKIE VIITLKENKG QRCLNPASAQ AALIIKKVER KNF
                                                  CLNPKSKQ AR
60s  FPMFKRGRCL CIGPGVKAVK VADIEKASIM YPSNNCDKIE VIITLKENKG QRCLNPKSKQ ARLIIAAVEA ANF
```

FIGURE 1. **Structure of CXCL11 and CXCL11 mutant sequences.** *A*, molecular modeling of the first NMR structure of CXCL11 in complex with a heparin endecasaccharide. Heparin is shown in *yellow*, and the basic residues predicted to be in contact with heparin are shown as *green sticks*. Predictions for the other NMR structures differ only in detail; all involve the 50s cluster, some involve the 60s cluster, and those (like the complex shown) where the unstructured N terminus happens to be in a favorable position also involve the N-terminal BB*X*B sequence. *B*, amino acid sequence of CXCL11 and the mutants. The mutated clusters are shown in *red*. Residues protected from tryptic digestion of the CXCL11-heparin complex are shown in *blue*. The additional residue predicted to participate in GAG binding by the molecular modeling, Lys^{17}, is shown in *green*, and was used in combination with the 50s cluster to generate 50s + K17A.

(^{66}AAVEAA^{71}) mutants. Following purification and renaturation, they were all found to be >95% pure as determined by SDS-PAGE and reverse phase HPLC (data not shown). The formation of the two disulfide bonds was confirmed by a shift in the reverse phase HPLC retention time and a loss of 4 Da by mass spectrometry (data not shown).

Molecular Modeling—In parallel, molecular docking calculations were used to predict amino acids that might be involved in GAG binding. A published protocol was used, which has been optimized for rapid identification of heparin binding sites on the surfaces of small proteins (33). In this protocol, docking of pentasaccharide ligands with flexible exocyclic bonds is used to identify the essential core of the heparin binding site on the protein, whereas docking with a rigid endecasaccharide can identify extended heparin binding sites. The protocol does not provide simulations of the bound complexes at atomic resolution. Conformational flexibility of the protein partner in this docking procedure cannot be addressed directly, but when an ensemble of protein structures is available from an NMR study, as in this case, it is possible to assess the effects of conformational flexibility on the location of the heparin binding site by docking to each set of coordinates in the ensemble. CXCL11 is a basic protein, with most of the arginine and lysine residues concentrated on one face, forming two strongly basic surface patches in which basic amino acids distant in sequence are close together in space. One of the patches includes Lys^{17}, Lys^{38}, Arg^{52}, Lys^{57}, Lys^{59}, and Arg^{62}. All 10 of the NMR structures were predicted by the docking calculations to interact with heparin by means of some residues in this patch, and for those structures in which the N-terminal BB*X*B motif is in close proximity, three basic residues (Lys^{5}, Arg^{6}, and Arg^{8}) are also predicted to be involved. Fig. 1 shows one of the CXCL11 NMR structures with the heparin endecasaccharide docked in the 10 lowest energy conformations. The second basic patch involves the residues Lys^{20}, Lys^{66}, Lys^{67}, Arg^{70}, and Lys^{71}, and for most of the predicted complexes, the endecasaccharide reaches Lys^{66} and sometimes Lys^{70}, but not Lys^{71} and Lys^{20}. Partially flexible heparin pentasaccharides docked with the first NMR structure occupied the first basic patch and the N terminus. Based on these docking results, we therefore made an additional mutant containing the 50s cluster plus K17A to more completely investigate the first basic patch. Fig. 1*B* shows the amino acid composition of each of the mutants compared with WT.

TABLE 1

Heparin affinity chromatography

The concentration (molar) of NaCl required for elution of the GAG binding mutants from heparin- and S-Sepharose columns compared with WT CXCL11 is indicated by $\Delta NaCl^{Hep}$ and $\Delta NaCl^{S}$, respectively. $\Delta\Delta$NaCl is the specificity index as described under "Experimental Procedures."

CXCL11	Heparin-Sepharose	S-Sepharose	$\Delta NaCl^{Hep}$	$\Delta NaCl^{S}$	$\Delta\Delta$NaCl
	M	*M*	*M*	*M*	*M*
WT	0.98	0.81			
10s	0.86	0.77	0.08	0.04	0.04
40s	0.81	0.68	0.17	0.13	0.04
50s	0.60	0.52	0.38	0.29	0.09
60s	0.77	0.68	0.21	0.13	0.08
50s + K17A	0.49	0.41	0.49	0.40	0.09

Heparin Binding Assays of CXCL11 Mutants Highlight the 50s Cluster as the Principle GAG Binding Epitope—Two assays were initially used to examine the GAG binding ability of the CXCL11 mutants. In both cases, we used heparin as a model GAG because it has been successfully used for many years for identifying GAG binding epitopes. Furthermore, as shown here and elsewhere (7, 21, 31, 38), the agreement between the *in vitro* and *in vivo* assays validates the use of heparin for this purpose. In the first assay, the NaCl concentration required to elute the mutant proteins from a heparin-Sepharose column was determined and compared with WT, yielding $\Delta NaCl^{Hep}$. Values of 0.38 and 0.49 for the 50s and 50s + K17A, respectively, suggest that these epitopes are more important contributors than the 60s, 40s, and 10s, which had values of 0.21, 0.17, and 0.08, respectively (Table 1), results that are largely in agreement with the modeling studies. The concentration of NaCl required for elution from a nonspecific S-Sepharose column was also determined in comparison with WT yielding $\Delta NaCl^{S}$. These values confirm the relative ordering of the mutants, as indicated by $\Delta NaCl^{Hep}$. $\Delta NaCl^{S}$ was then subtracted from $\Delta NaCl^{Hep}$ to eliminate nonspecific electrostatic contributions, yielding $\Delta\Delta$NaCl, which effectively provides a measure of the specificity of a given amino acid for heparin. Thus, a greater effect of the mutations on specific heparin binding is reflected by more positive $\Delta\Delta$NaCl values. Both the 50s epitope and 50s + K17A had $\Delta\Delta$NaCl values of 0.09, the 60s epitope had a $\Delta\Delta$NaCl of 0.08, and the 10s and 40s epitopes had a $\Delta\Delta$NaCl of 0.04, suggesting the highest specificity for the 50s cluster (Table 1). Although the 60s was a close second, the overall affinity as defined by $\Delta[NaCl]^{Hep}$ and $\Delta[NaCl]^{S}$ suggests that it is less important than the 50s.

The second assay consisted of direct binding measurements of the proteins to heparin immobilized on specialized plates, with bound protein detected by a polyclonal antibody. The EC_{50} values for the WT, 10s, and 60s mutants were very similar

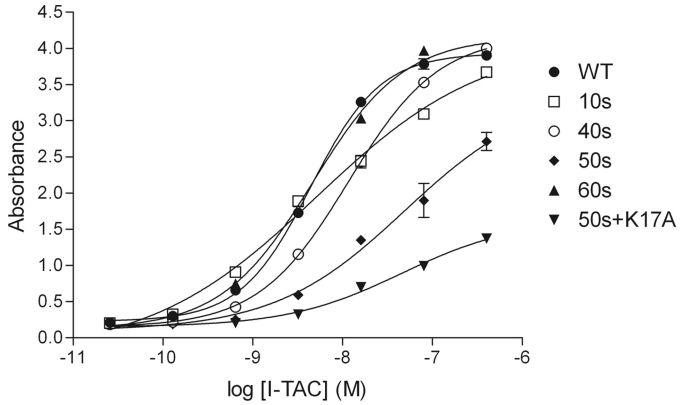

FIGURE 2. **Comparison of the ability of WT CXCL11 and the mutants to bind to heparin immobilized on Epranex plates.** Although WT and the 10s and 60s mutants show similar EC_{50} values, the value for the 40s mutant is slightly reduced, and the 50s mutant shows a 10-fold lower EC_{50} as well as reduced binding capacity. The addition of K17A to the 50s cluster shows a further reduction in EC_{50} and binding capacity. *Error bars*, S.D.

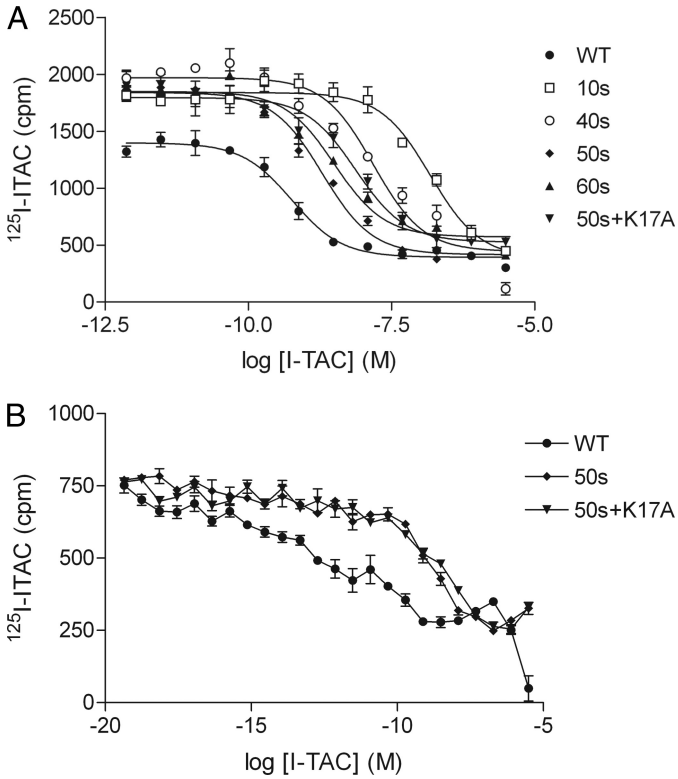

FIGURE 3. **Equilibrium competition receptor binding assays.** *A*, a dilution series of competitor was prepared down to picomolar concentrations of competitor ligand. The rank ordering of the IC_{50} values is as follows: 10s (225-fold loss relative to WT) > 40s (30-fold loss) > 50s + K17A (7-fold loss) ~ 60s (6-fold loss) ~ 50s (3-fold loss). *B*, because WT CXCL11 reproducibly showed a 30–50% lower number of total counts representing bound [^{125}I]CXCL11, at the lowest concentrations of competitor in *A*, the measurements were extended to subpicomolar competitor concentrations. *Error bars*, S.D.

(3.38 ± 1.05, 3.75 ± 1.67, and 3.76 ± 1.06 nM, respectively), the 40s mutant was intermediate (8.54 ± 3.76), and the 50s mutant showed a 10-fold decrease (38.8 ± 18.10 nM) relative to WT. Interestingly, as shown in Fig. 2, the 50s mutant showed a 50% reduction in binding capacity, and when combined with K17A, the binding capacity decreased to 30%. Possible reasons for this behavior will be discussed later. Nevertheless, these data further support a dominant contribution to GAG binding by the combination of the 50s + K17.

In parallel with the above studies, a proteolytic protection assay was undertaken. Proteolytic footprinting allows for the identification of regions of a protein that bind to GAGs without the requirement for mutagenesis. The protein of interest, complexed to a GAG, is subject to digestion with trypsin. The resulting peptides are subsequently analyzed by mass spectrometry and compared with those obtained after a digest of the free protein (35). Regions that are complexed with the GAG are protected from digestion and are thus identified in comparison with digests in the absence of heparin (or other GAG). This method was used to confirm the GAG binding site of CXCL11 as being principally located in a region encompassing the 50s loop (^{53}CLNPKSKQAR^{62}) because this region was digested in the absence of heparin but remained intact in the presence of heparin (supplemental Fig. 1, *A* and *B*). Detected ions had masses of 1145.45 (single charged) and 573.20 (double charged), which correspond to molecular weights of 1144.45 (single charged) and 1144.40 (double charged) and compare well with the calculated molecular weight of 1144.36. Strong protection was not observed anywhere else. Although our data suggest the importance of Lys^{17}, one would not necessarily expect to be able to detect protection of this residue in a proteolytic footprinting assay. It is not associated with a large sequential cluster, which might be required to observe significant protection, and it is distant in sequence from the 50s epitope.

Competition Receptor Binding Assays Indicate that the 50s Cluster plus Lys^{17} Contribute Little to Receptor Binding Affinity and Receptor Activation—The ultimate tests of the relevance of GAG binding and the identification of binding epitopes are *in vivo* assays of cell recruitment. As a prelude to these studies, however, it is critical to determine whether mutations that affect GAG binding also impact receptor binding and activation for accurate interpretation of the *in vivo* results. Accordingly, the receptor binding affinities of the mutants for CXCR3 were determined in comparison with the WT protein using an SPA-based competition binding assay with CHO membranes expressing CXCR3 (Fig. 3*A*). Our recombinant WT CXCL11 was compared with the commercially available CXCL11 protein obtained from PeproTech, and both proteins yielded similar results, with IC_{50} values of 0.3 and 0.6 nM (results not shown). The mutants were all able to compete for the iodinated WT protein albeit with varying affinities. The most pronounced loss of affinity was seen for the 10s mutant, which had an IC_{50} of 102 ± 61 nM, representing a 225-fold loss compared with WT (based on the mean WT value of 0.45 nM). This observation is consistent with the importance of the amino terminus in receptor binding (and signaling) for all chemokines reported to date. More specifically, the basic residue, Arg^8, in the N terminus of CXCL10 has been shown to play a role in binding to CXCR3 (39), and this residue is also an Arg in CXCL11. For the 40s mutant, the IC_{50} value was determined to be 13.7 ± 2.75 nM, which corresponds to a 30-fold loss of affinity, suggesting that the 40s loop is involved in receptor binding. The 50s and 60s mutants showed little loss of affinity, with IC_{50} values of 1.3 ± 1.0 and 2.6 ± 0.5 nM, respectively, corresponding to only 3- and

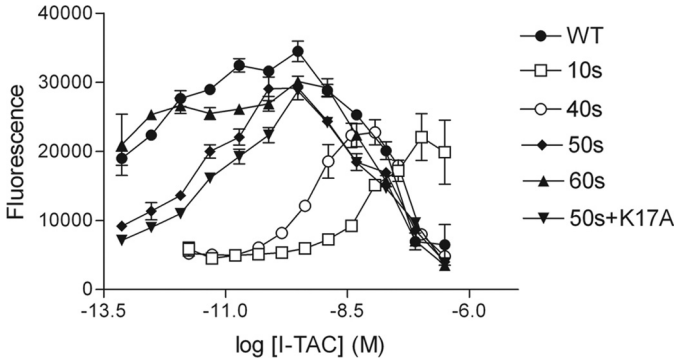

FIGURE 4. ***In vitro* chemotaxis assay.** In accordance with its inability to bind the receptor, the 10s mutant shows significantly impaired chemotactic potency, 400-fold lower than WT. The maximum of the chemotactic response for the 40s mutant is shifted to 20 times higher concentration relative to WT CXCL11. The 50s, 60s, and 50s + K17A mutants, on the other hand, showed chemotactic behavior comparable with that of WT CXCL11. *Error bars*, S.D.

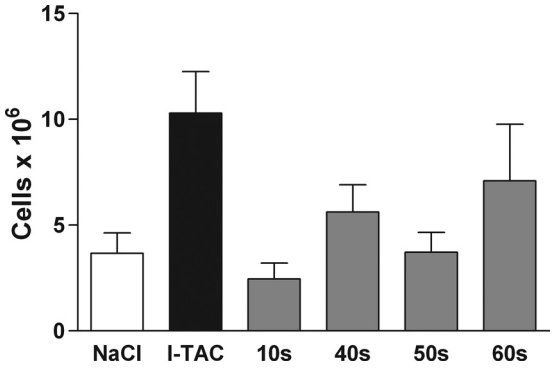

FIGURE 5. **Ability of the CXCL11 mutants to recruit cells into the peritoneal cavity.** The 10s and 40s mutants show a highly impaired ability to recruit cells to the peritoneum, as expected from the effect of the mutations on receptor binding. The inability of the 50s mutant to recruit cells, on the other hand, is due to its impaired GAG binding. *Error bars*, S.D.

6-fold drops. Introduction of K17A into the 50s mutant caused a further 3-fold reduction of affinity with an IC_{50} value of 3.0 ± 3.9 nM.

One of the most intriguing findings, observed in five separate experiments, was that both the commercial CXCL11 and our recombinant protein had 30–50% lower [^{125}I]CXCL11 bound to the membrane-coated beads compared with the mutants at the lowest picomolar competitor concentrations used in Fig. 3*A*. This suggested the presence of an even higher affinity binding mode for the WT protein that was eliminated by the mutations. We therefore extended the competition binding experiments to lower concentrations of cold competitor, including a control with no cold chemokine added. Importantly, these curves all converge at the lowest concentrations, and they do indeed show the presence of a subpicomolar interaction that represents ~30–50% of the total binding for the WT protein (Fig. 3*B*).

The ability of the CXCL11 mutants to activate CXCR3 was further assessed with a chemotaxis assay using L1.2 cells expressing CXCR3. The 50s, 60s, and 50s + K17A mutants demonstrated equivalent potency to the WT, with a maximal response at 0.3 nM, consistent with a minimal perturbation of receptor binding. In accordance with its loss of affinity for the receptor, the 10s mutant showed significantly impaired recruitment of CXCR3-expressing cells with a 50% loss in efficacy and 400-fold loss of potency such that 125 nM ligand was required to achieve the maximal response (Fig. 4). Paralleling the 30-fold loss of affinity for CXCR3, the 40s loop mutant required 7 nM ligand for the maximal response (20-fold lower than the WT), and the efficacy was 50% of WT. Considering all of the data, the 50s and 50s + K17A mutants showed the least perturbation on receptor binding and activation but the largest effect on GAG binding, making them particularly suitable for evaluating the role of GAG binding and the importance of these epitopes *in vivo*.

An in Vivo Peritoneal Cellular Recruitment Assay Confirms the Importance of GAG Binding and the 50s Epitope for the Chemotactic Activity of CXCL11—The ability of the cluster mutants to attract cells *in vivo* relative to WT CXCL11 was examined in a T cell peritoneal recruitment assay. Because CXCR3 is only expressed on activated T cells, the mice were sensitized with CpG prior to the assay (40). Interestingly, most of the mutants showed impaired cell recruitment compared with WT CXCL11, although the small reduction observed for the 60s was not statistically significant and indicates that it contributes little to GAG binding (Fig. 5). The inability of the 10s and 40s mutants to recruit cells in the *in vivo* assay was expected, based on the *in vitro* binding and chemotaxis assays. However, because the 50s loop mutant showed a WT chemotaxis profile and little difference in affinity for the receptor relative to WT CXCL11, the inability to recruit cells *in vivo* can only be attributed to the defect in GAG binding. In fact, although the 40s mutant was significantly impaired in the *in vitro* chemotaxis assay relative to the 50s mutant, it was capable of recruiting more cells than the 50s mutant, further emphasizing the relevance of the 50s region and not the 40s on GAG binding. These *in vivo* data are also remarkably consistent with the *in vitro* data, despite the use of heparin as a surrogate for heparin sulfate or other GAGs for identification of the GAG-binding epitopes.

An Immobilized Heparin Assay Defines a High Affinity GAG Site—In principle, the picomolar binding site identified in the equilibrium receptor binding assay may represent a high affinity site on CXCR3, another receptor, or a GAG site. To investigate the potential role of a high affinity GAG site, we conducted a solid phase binding assay on heparin beads, extending the concentration range of the heparin from 10^{-6} to 10^{-15} M. Surprisingly, a high affinity binding site was in fact observed (Fig. 6*A*). Using average molecular weights as outlined under "Experimental Procedures," the high affinity sites correspond to an IC_{50} of ~100 pM for the 3-kDa heparin (H3400) and 13 pM for unfractionated heparin (H3393, 5–30 kDa). These numbers are obviously only approximations and rest on the additional assumption that there is only one binding site per chain (which is probably true for 3-kDa heparin (~10 monosaccharides) but not unfractionated heparin); thus, the data are plotted as mg/ml. Nevertheless, although approximate, they do suggest an unusually high affinity of heparin for CXCL1l. In view of this unexpected observation, we tested CCL5 in this assay, and observed the same phenomenon: a high affinity site with an IC_{50} of 20 pM for 3-kDa heparin and 2 pM for unfractionated heparin, in addition to the well characterized low affinity site

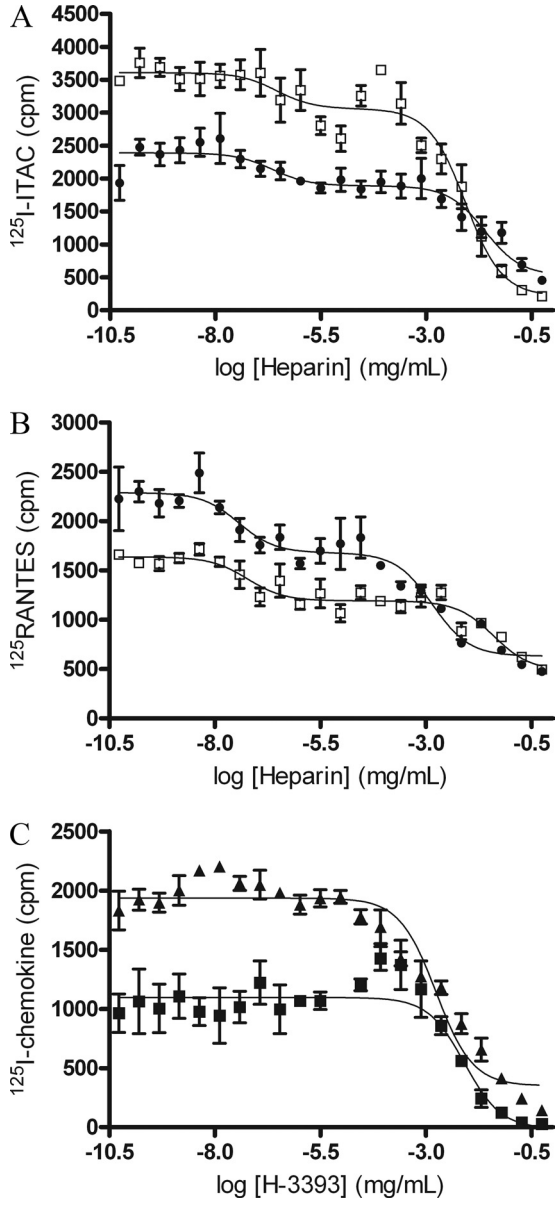

FIGURE 6. **Immobilized heparin competition binding assay.** In an immobilized heparin competition binding assay, the chemokines CXCL11 and CCL5 show a second, high affinity binding site with unfractionated heparin (H3393) as well as with low molecular weight heparin (H3400) as the competitor. *A*, CXCL11 with H3393 (*filled circles*) and H3400 (*open squares*). *B*, CCL5 with H3393 (*filled circles*) and H3400 (*open squares*). *C*, SDF-1/CXCL12 (*triangles*) and MCP-1/CCL2 (*filled squares*) do not show the high affinity binding site with unfractionated (H3393) heparin. Note, the differences in the absolute cpm values are due to the experiments being conducted at different times and are unimportant. *Error bars*, S.D.

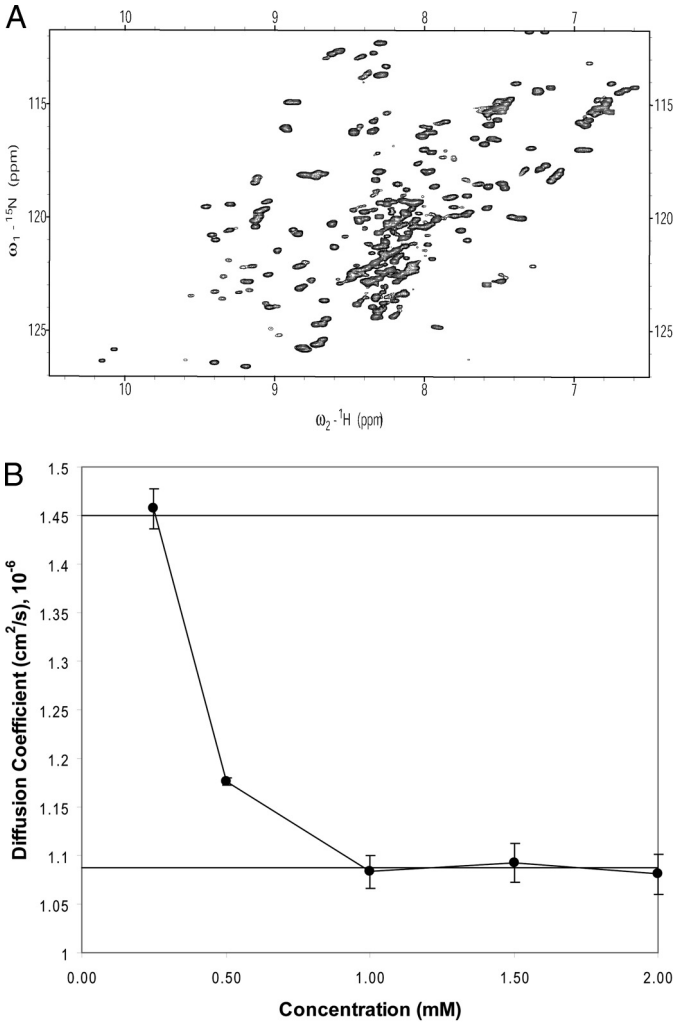

FIGURE 7. *A*, ^{1}H-^{15}N HSQC spectra of CXCL11. The data show the presence of two and in some cases three species interconverting in slow exchange. Note for example the two cross-peaks between 10 and 10.2 ppm. *B*, pulsed field gradient diffusion profile of WT CXCL11 over a range of concentrations from 0.25 to 2.0 mM. The *lines* indicate the diffusion for the monomer and dimer; assuming the diffusion coefficient at 0.25 mM corresponds to the monomeric form, the theoretical D_s value for the dimer was estimated using the Stokes-Einstein equation as 1.09×10^{-10} m^2/s.

with an IC_{50} of 0.15 μM (Fig. 6*B*). However, no obvious high affinity binding sites were observed for CCL2 and CXCL12, where the IC_{50} values for competition by heparin were more typical, at 0.34 and 0.14 μM, respectively (Fig. 6*C*).

NMR Studies of CXCL11 Indicate That It Forms a Dimer and Is Conformationally Heterogeneous in Solution—To corroborate the above results, we intended to use chemical shift perturbation experiments with heparin fragments of defined size and composition. To this end, we prepared ^{15}N-labeled CXCL11 and recorded HSQC spectra at various temperatures and pH conditions. However, unlike most other chemokines, CXCL11 showed evidence of multiple species in slow exchange, by the presence of more cross-peaks than one would expect, with most peaks at least doubled and in some cases tripled (Fig. 7). Pulsed field gradient diffusion NMR experiments (41) indicate that CXCL11 is a dimer under the conditions used for the HSQC (Fig. 7*B*). These results and the uniform size of the cross-peaks suggest that the extra peaks are not due to the presence of both monomer and dimer but rather alternate conformations of the chemokine. This behavior is consistent with a previous report on the NMR structure of CXCL11, which was determined at low pH (4.5) and high temperature (40 °C) because only these conditions gave a single species (34). Because of the complexity of the spectra under most conditions, we abandoned the chemical shift perturbation experiments, which would require challenging spectral assignments. Nevertheless, the results are intriguing and suggest some unique conformational plasticity for this chemokine, which could be related to the observation of

high affinity binding sites in the SPA receptor binding assay and in the immobilized heparin assay.

Attempts were made to determine if CXCL11 oligomerizes further in solution in the presence of heparin, as observed for CCL2 (31) and CCL27 (62). However, the addition of heparin octasaccharide caused immediate precipitation of the complex at substoichiometric concentrations of GAG to chemokine (supplemental Fig. 2). Although this behavior makes it difficult to characterize the oligomeric state of CXCL11 in the complex, similar behavior was observed for CCL2, although it did not precipitate as vigorously, and what was left in solution was tetrameric (62). Heparin octasaccharide has also been shown to stabilize oligomerization of several other CCR2 ligands as both homo- and hetero-oligomers (42). Thus, it seems likely that GAGs stabilize the CXCL11 dimer and induce higher order oligomerization.

DISCUSSION

The interactions of chemokines with cell surface GAGs, in addition to high affinity interactions with their receptors on leukocytes, play an essential role in cell recruitment. This has been demonstrated *in vivo* using chemokine mutants that have a compromised ability to bind GAGs *in vitro* but intact receptor binding; although such GAG binding-deficient mutants are generally competent to recruit cells *in vitro* in simple trans-well assays, they are incapable of inducing migration *in vivo* (7, 38). The requirement for the GAG interaction is thought to reflect, in part, the need for the sequestration of chemokines on cell surfaces, where they provide directional cues for migrating cells. Indeed, a mutant of RANTES, ^{44}AANA^{47}-RANTES, rapidly accumulates in serum when injected intraperitoneally, in contrast to the WT protein (43). Notably, this mutant was able to block the *in vivo* cell recruitment to the WT protein and was shown to be effective in three murine models of inflammation (thioglycollate- and ovalbumin-induced cell recruitment and MOG-induced experimental autoimmune encephalomyelitis). Similarly, a GAG-binding mutant of MCP-3/CCL7 antagonizes chemokine-mediated cell recruitment in an air pouch *in vivo* model and *in vitro* to the synovial fluid from patients with rheumatoid arthritis (38). Finally, a GAG-binding mutant of CCL2 inhibits recruitment of cells to WT CCL2 in an *in vivo* peritoneal recruitment assay.[4] Because there are ~50 ligands in the human chemokine system, it remains to be seen if GAG binding is important for the vast majority of the ligands. The chemokine family also provides an extraordinary opportunity for investigating the extent to which GAG interactions add to the specificity of their function. Finally, the ability of GAG mutants to antagonize chemokine function offers the potential for the development of novel therapeutics.

For these reasons, in this study, we set out to define the GAG binding determinants of the chemokine I-TAC/CXCL11. CXCL11 mutants were prepared and tested in several *in vitro* assays of GAG binding, including the commonly used method of heparin affinity chromatography in conjunction with cation exchange chromatography, and in an Epranex plate assay. These assays provide a relative quantitative measure of affinity rather than absolute binding constants, which would require a completely homogeneous GAG with a single or known number of binding sites, entities that are not readily available. However taken together, these assays defined Lys^{57}, Lys^{59}, and Arg^{62} in the 50s region and Lys^{17} as forming the dominant GAG-binding epitope. Furthermore, the protease protection assay confirmed the importance of the 50s epitope.

Lortat-Jacob *et al.* (44, 45) describe the existence of typical GAG binding sites for each chemokine class. They state that for most CXC chemokines, the residues of the C-terminal helix together with residues connecting the first N-terminal β-strand with the N terminus are involved. We examined the positions of the mutated residues of the 50s mutant and Lys^{17} and found that they exactly coincide with the binding site predicted (supplemental Fig. 3). Matrix metalloproteases 8, 9, and 12 process CXCL11 at both the N and C terminus to generate CXCL11(5–73), CXCL11(5–63), and CXCL11(5–58), where processing of the amino terminus results in increased GAG binding, and C-terminal truncation results in the loss of GAG binding (46). Although one cannot exclude an indirect effect from misfolding, the results from C-terminal truncation correlate with our findings that the 50s cluster (^{57}KSKQAR^{62}) is involved in GAG binding because two of the basic residues are removed.

The ultimate test of the importance of a GAG binding motif is *in vivo* recruitment. For reliable interpretation of these experiments, a requirement is that the mutations do not significantly perturb the ability of the chemokine to bind and activate its receptor. As seems to be the case for many chemokines, although there is often some overlap in GAG and receptor binding sites, one can usually identify mutations that impair GAG binding without significantly interfering with receptor binding and signaling. The interaction of CCL5 with CCR5 is a good example, where complete decoupling of the receptor and GAG-binding epitopes are observed, although this is not the case for CCL5 and CCR1. CCL2 is another good example, where GAG-binding and receptor-binding epitopes can be distinguished because only a 20-fold loss in affinity for CCR2 was observed with the GAG-binding mutant ^{18}AA^{19}-MCP-1, and the mutant showed equal efficacy to the WT chemokine in cell migration (4). Perhaps the best example is a GAG-binding mutant of CCL7, which actually showed slightly higher affinity for the receptor compared with the WT chemokine (38). Similarly, the CXCL11 50s + Lys^{17} mutant, which bound heparin poorly *in vitro*, showed only a small decrease in receptor binding, and the efficacy and potency for inducing cell migration was equivalent to the WT protein. Consequently, the reduced ability of the 50s mutant to induce cell recruitment into the peritoneal cavity establishes these residues as *bona fide* contributors to GAG binding. By contrast, the inability of the 10s mutant to recruit cells is due to the substantial effect of the mutations on receptor binding and activation, and by contrast, these mutated residues contribute little to GAG binding, despite conforming to a classic BB*X*B motif. The 40s cluster also contributes more to receptor binding/signaling and less to GAG binding compared with the 50s epitope and 50s + Lys^{17}. Although it remains to be determined, the ability to fully or partially decouple GAG binding from signaling may have impli-

[4] Z. Johnson, A. E. I. Proudfoot, and T. Handel, unpublished data.

cations for whether or not chemokines can simultaneously bind to GAGs and receptors or whether the interactions are mutually exclusive. These *in vivo* observations confirm the results of our *in vitro* assays and furthermore validate the use of heparin as a suitably representative GAG for defining GAG epitopes.

An emerging theme in the chemokine field is that GAG binding epitopes are often not confined to linear epitopes like BB*X*B because some chemokines oligomerize on GAGs, making much more diffuse sites in the context of the quaternary structures (6). The 50s + Lys^{17} motif constitutes a diffuse site in the tertiary structure of CXCL11 but would present a different surface again in the context of the dimer or higher order oligomer. The principal GAG binding residues of another CXCR3 ligand, IP-10/CXCL10, are situated in the 20s and 40s loops (39), suggesting significant differences from CXCL11 and underlying specificity between these chemokines with respect to GAG binding. Although its NMR structure was solved as a monomer (47), human CXCL10 has been crystallized in three different tetrameric forms that have been suggested to be involved in GAG binding (48), and a recent structure of murine CXCL10 reveals yet a fourth tetrameric form (49). Although dimeric in solution, MCP-1/CCL2 forms tetramers, as shown by crystallography (50), and the tetramer is stabilized by the presence of GAGs (31). PF-4/CXCL4 also crystallizes as a tetramer and forms tetramers in solution (51, 52), whereas RANTES/CCL5 forms large oligomeric structures, which can be destabilized into dimers and tetramers by point mutations (53). The structure of CXCL11 was solved as a monomer by NMR because of the low pH conditions used for the sample preparation (34); however, this chemokine clearly dimerizes in solution under more physiological conditions (Fig. 7*B*) and, like other chemokines, such as CCL2, may oligomerize further in the presence of GAGs (supplemental Fig. 2). Reduced stabilization of oligomers by GAGs for the mutants relative to WT is the most likely explanation for the lower binding capacity of the GAG mutants in the solid phase heparin assay compared with WT in Fig. 2.

Although oligomeric structures of CXCL10 have been solved by crystallography, crystallizing CXCL11 has not been feasible.[5] The spectra shown in Fig. 7, however, provide an obvious explanation for why crystallization has been challenging; CXCL11 is conformationally heterogeneous. This heterogeneous behavior is likely to be relevant to its biological function involving different receptor and/or GAG interactions. Although most chemokines studied to date appear to adopt a single conformation based on their HSQC spectra, another example of structural promiscuity has been reported for the human chemokine lymphotactin/XCL1. Similar to CXCL11, the HSQC spectra of XCL1 are indicative of two species, and in fact, XCL1 exists in equilibrium between two entirely distinct folds: one that binds GAGs but does not bind or activate the receptor and one that has the complementary receptor binding ability but does not bind GAGs (54). CXCL11 may also be subject to dynamic structural interconversion, although it is not likely to be as extreme as lymphotactin because the CXCL11 structure is locked down by two disulfides, whereas XCL1 has only a single disulfide bond. Nevertheless, it is likely to be biologically relevant, and we are currently investigating the structural nature and functional significance of this behavior in CXCL11.

Two unusual observations made in the current study may be related to the conformational heterogeneity of CXCL11, however. The receptor binding studies revealed a consistent anomaly in at least five repetitive experiments, in that the WT protein showed a reduced binding capacity for CXCR3 compared with the mutants, as judged by the radioactivity counts at picomolar concentrations. We therefore used even lower concentrations of competitor and identified a subpicomolar interaction that represents ~30–50% of the total. This interaction could involve CXCR3, another receptor, or a GAG interaction. The presence of more than one binding site could also reflect the structural heterogeneity of CXCL11, where one conformation displays a higher affinity than the other. To address this observation, we posed the question of whether GAG binding could account for the high affinity interaction, with an assay consisting of competition of radiolabeled CXCL11 to immobilized heparin, extending the concentration of unlabeled CXCL11 to femtomolar concentrations. Effectively, a very high affinity site was revealed. We then tested CCL2, CCL5, and CXCL12 in a similar assay and observed the same phenomenon for CCL5 but not for CCL2 and CXCL12, with the most pronounced effect observed for CXCL11. Because GAGs are heterogeneous, the valency of the interaction is unknown, and the molecular weights for the GAGs are average values. Therefore, it is not possible to obtain exact IC_{50} values. However, there is no doubt that CXCL11 and CCL5 have unusually high affinities compared with other chemokines. Moreover it will be interesting to investigate whether the high affinity site exits for other GAGs, such as heparan sulfate, chondroitin sulfate, and dermatan sulfate, in addition to heparin.

In summary, it is clear that GAG binding plays an important role in CXCL11 function and that binding sites comparable in affinity to receptors do exist. In this study, we characterized a GAG-binding mutant of CXCL11 that consists of mutations that are largely separate from the receptor binding determinants. Although we have not tested the GAG-binding mutant as an inhibitor of cell migration *in vivo* or in disease models, the results described above for CCL5 and CCL7 GAG mutants suggest that one can anticipate that the 50s + Lys^{17} mutant will also be an effective antagonist of cell migration. The most widely appreciated chemokine-based antagonists consist of chemokines in which the N terminus is modified in some way by mutation, deletion, or extension (55, 56). Non-oligomerizing chemokines have also been shown to be powerful inhibitors of cell migration in experimental autoimmune encephalomyelitis and rheumatoid arthritis (57, 58). GAG binding-deficient chemokines offer a third possibility. A GAG-binding mutant of CCL5 functions at least in part by a dominant negative mechanism involving formation of heterodimers and preventing higher order oligomerization (43). As suggested in recent studies, GAG-binding mutants that retain their agonist properties may be

[5] J. P. Shaw, personal communication.

particularly effective and even have broad spectrum effects due to homologous and heterologous desensitization (38, 59, 60). Herein we have defined a GAG-binding mutant of CXCL11 that retains its agonist activity and can be used in future studies to test its efficacy in the many inflammatory diseases where CXCR3 and its ligands have been implicated (61).

REFERENCES

1. Mackay, C. R. (2001) *Nat. Immunol.* **2,** 95–101
2. Sallusto, F., and Baggiolini, M. (2008) *Nat. Immunol.* **9,** 949–952
3. Laurence, J. S., Blanpain, C., Burgner, J. W., Parmentier, M., and LiWang, P. J. (2000) *Biochemistry* **39,** 3401–3409
4. Paavola, C. D., Hemmerich, S., Grunberger, D., Polsky, I., Bloom, A., Freedman, R., Mulkins, M., Bhakta, S., McCarley, D., Wiesent, L., Wong, B., Jarnagin, K., and Handel, T. M. (1998) *J. Biol. Chem.* **273,** 33157–33165
5. Rajarathnam, K., Sykes, B. D., Kay, C. M., Dewald, B., Geiser, T., Baggiolini, M., and Clark-Lewis, I. (1994) *Science* **264,** 90–92
6. Handel, T. M., Johnson, Z., Crown, S. E., Lau, E. K., and Proudfoot, A. E. (2005) *Annu. Rev. Biochem.* **74,** 385–410
7. Proudfoot, A. E., Handel, T. M., Johnson, Z., Lau, E. K., LiWang, P., Clark-Lewis, I., Borlat, F., Wells, T. N., and Kosco-Vilbois, M. H. (2003) *Proc. Natl. Acad. Sci. U.S.A.* **100,** 1885–1890
8. Bacon, K., Baggiolini, M., Broxmeyer, H., Horuk, R., Lindley, I., Mantovani, A., Maysushima, K., Murphy, P., Nomiyama, H., Oppenheim, J., Rot, A., Schall, T., Tsang, M., Thorpe, R., Van Damme, J., Wadhwa, M., Yoshie, O., Zlotnik, A., and Zoon, K. (2002) *J. Interferon Cytokine Res.* **22,** 1067–1068
9. Kuschert, G. S., Coulin, F., Power, C. A., Proudfoot, A. E., Hubbard, R. E., Hoogewerf, A. J., and Wells, T. N. (1999) *Biochemistry* **38,** 12959–12968
10. Liu, D., Shriver, Z., Venkataraman, G., El Shabrawi, Y., and Sasisekharan, R. (2002) *Proc. Natl. Acad. Sci. U.S.A.* **99,** 568–573
11. Sasisekharan, R., Shriver, Z., Venkataraman, G., and Narayanasami, U. (2002) *Nat. Rev. Cancer* **2,** 521–528
12. Shriver, Z., Liu, D., and Sasisekharan, R. (2002) *Trends Cardiovasc. Med.* **12,** 71–77
13. Vlodavsky, I., Goldshmidt, O., Zcharia, E., Atzmon, R., Rangini-Guatta, Z., Elkin, M., Peretz, T., and Friedmann, Y. (2002) *Semin. Cancer Biol.* **12,** 121–129
14. Johnson, Z., Proudfoot, A. E., and Handel, T. M. (2005) *Cytokine Growth Factor Rev.* **16,** 625–636
15. Amara, A., Lorthioir, O., Valenzuela, A., Magerus, A., Thelen, M., Montes, M., Virelizier, J. L., Delepierre, M., Baleux, F., Lortat-Jacob, H., and Arenzana-Seisdedos, F. (1999) *J. Biol. Chem.* **274,** 23916–23925
16. Hemmerich, S., Paavola, C., Bloom, A., Bhakta, S., Freedman, R., Grunberger, D., Krstenansky, J., Lee, S., McCarley, D., Mulkins, M., Wong, B., Pease, J., Mizoue, L., Mirzadegan, T., Polsky, I., Thompson, K., Handel, T. M., and Jarnagin, K. (1999) *Biochemistry* **38,** 13013–13025
17. Jarnagin, K., Grunberger, D., Mulkins, M., Wong, B., Hemmerich, S., Paavola, C., Bloom, A., Bhakta, S., Diehl, F., Freedman, R., McCarley, D., Polsky, I., Ping-Tsou, A., Kosaka, A., and Handel, T. M. (1999) *Biochemistry* **38,** 16167–16177
18. Koopmann, W., and Krangel, M. S. (1997) *J. Biol. Chem.* **272,** 10103–10109
19. Kuschert, G. S., Hoogewerf, A. J., Proudfoot, A. E., Chung, C. W., Cooke, R. M., Hubbard, R. E., Wells, T. N., and Sanderson, P. N. (1998) *Biochemistry* **37,** 11193–11201
20. Peterson, F. C., Elgin, E. S., Nelson, T. J., Zhang, F., Hoeger, T. J., Linhardt, R. J., and Volkman, B. F. (2004) *J. Biol. Chem.* **279,** 12598–12604
21. Proudfoot, A. E., Fritchley, S., Borlat, F., Shaw, J. P., Vilbois, F., Zwahlen, C., Trkola, A., Marchant, D., Clapham, P. R., and Wells, T. N. (2001) *J. Biol. Chem.* **276,** 10620–10626
22. Sadir, R., Baleux, F., Grosdidier, A., Imberty, A., and Lortat-Jacob, H. (2001) *J. Biol. Chem.* **276,** 8288–8296
23. Cole, K. E., Strick, C. A., Paradis, T. J., Ogborne, K. T., Loetscher, M., Gladue, R. P., Lin, W., Boyd, J. G., Moser, B., Wood, D. E., Sahagan, B. G., and Neote, K. (1998) *J. Exp. Med.* **187,** 2009–2021
24. Flier, J., Boorsma, D. M., van Beek, P. J., Nieboer, C., Stoof, T. J., Willemze, R., and Tensen, C. P. (2001) *J. Pathol.* **194,** 398–405
25. Sauty, A., Dziejman, M., Taha, R. A., Iarossi, A. S., Neote, K., Garcia-Zepeda, E. A., Hamid, Q., and Luster, A. D. (1999) *J. Immunol.* **162,** 3549–3558
26. Sauty, A., Colvin, R. A., Wagner, L., Rochat, S., Spertini, F., and Luster, A. D. (2001) *J. Immunol.* **167,** 7084–7093
27. Qin, S., Rottman, J. B., Myers, P., Kassam, N., Weinblatt, M., Loetscher, M., Koch, A. E., Moser, B., and Mackay, C. R. (1998) *J. Clin. Invest.* **101,** 746–754
28. Loetscher, P., Pellegrino, A., Gong, J. H., Mattioli, I., Loetscher, M., Bardi, G., Baggiolini, M., and Clark-Lewis, I. (2001) *J. Biol. Chem.* **276,** 2986–2991
29. Burns, J. M., Summers, B. C., Wang, Y., Melikian, A., Berahovich, R., Miao, Z., Penfold, M. E., Sunshine, M. J., Littman, D. R., Kuo, C. J., Wei, K., McMaster, B. E., Wright, K., Howard, M. C., and Schall, T. J. (2006) *J. Exp. Med.* **203,** 2201–2213
30. Hoogewerf, A. J., and Kuschert, G. S. (2000) *Methods Mol. Biol.* **138,** 173–177
31. Lau, E. K., Paavola, C. D., Johnson, Z., Gaudry, J. P., Geretti, E., Borlat, F., Kungl, A. J., Proudfoot, A. E., and Handel, T. M. (2004) *J. Biol. Chem.* **279,** 22294–22305
32. Hamel, D. J., Sielaff, I., Proudfoot, A. E., and Handel, T. M. (2009) *Methods Enzymol.* **461,** 71–102
33. Mulloy, B., and Forster, M. J. (2008) *Mol. Simul.* **34,** 481–489
34. Booth, V., Clark-Lewis, I., and Sykes, B. D. (2004) *Protein Sci.* **13,** 2022–2028
35. Falsone, S. F., Gesslbauer, B., Rek, A., and Kungl, A. J. (2007) *Proteomics.* **7,** 2375–2383
36. Chung, C. W., Cooke, R. M., Proudfoot, A. E., and Wells, T. N. (1995) *Biochemistry* **34,** 9307–9314
37. Altieri, A. S., Hinton, D. P., and Byrd, R. A. (1995) *J. Am. Chem. Soc.* **117,** 7566–7567
38. Ali, S., Robertson, H., Wain, J. H., Isaacs, J. D., Malik, G., and Kirby, J. A. (2005) *J. Immunol.* **175,** 1257–1266
39. Campanella, G. S., Lee, E. M., Sun, J., and Luster, A. D. (2003) *J. Biol. Chem.* **278,** 17066–17074
40. Langenkamp, A., Nagata, K., Murphy, K., Wu, L., Lanzavecchia, A., and Sallusto, F. (2003) *Eur. J. Immunol.* **33,** 474–482
41. Dehner, A., and Kessler, H. (2005) *Chembiochem* **6,** 1550–1565
42. Crown, S. E., Yu, Y., Sweeney, M. D., Leary, J. A., and Handel, T. M. (2006) *J. Biol. Chem.* **281,** 25438–25446
43. Johnson, Z., Kosco-Vilbois, M. H., Herren, S., Cirillo, R., Muzio, V., Zaratin, P., Carbonatto, M., Mack, M., Smailbegovic, A., Rose, M., Lever, R., Page, C., Wells, T. N., and Proudfoot, A. E. (2004) *J. Immunol.* **173,** 5776–5785
44. Lortat-Jacob, H., Grosdidier, A., and Imberty, A. (2002) *Proc. Natl. Acad. Sci. U.S.A.* **99,** 1229–1234
45. Laguri, C., Arenzana-Seisdedos, F., and Lortat-Jacob, H. (2008) *Carbohydr. Res.* **343,** 2018–2023
46. Cox, J. H., Dean, R. A., Roberts, C. R., and Overall, C. M. (2008) *J. Biol. Chem.* **283,** 19389–19399
47. Booth, V., Keizer, D. W., Kamphuis, M. B., Clark-Lewis, I., and Sykes, B. D. (2002) *Biochemistry* **41,** 10418–10425
48. Swaminathan, G. J., Holloway, D. E., Colvin, R. A., Campanella, G. K., Papageorgiou, A. C., Luster, A. D., and Acharya, K. R. (2003) *Structure* **11,** 521–532
49. Jabeen, T., Leonard, P., Jamaluddin, H., and Acharya, K. R. (2008) *Acta Crystallogr. D Biol. Crystallogr.* **64,** 611–619
50. Lubkowski, J., Bujacz, G., Boqué, L., Domaille, P. J., Handel, T. M., and Wlodawer, A. (1997) *Nat. Struct. Biol.* **4,** 64–69
51. Mayo, K. H., and Chen, M. J. (1989) *Biochemistry* **28,** 9469–9478
52. Zhang, X., Chen, L., Bancroft, D. P., Lai, C. K., and Maione, T. E. (1994) *Biochemistry* **33,** 8361–8366
53. Czaplewski, L. G., McKeating, J., Craven, C. J., Higgins, L. D., Appay, V., Brown, A., Dudgeon, T., Howard, L. A., Meyers, T., Owen, J., Palan, S. R., Tan, P., Wilson, G., Woods, N. R., Heyworth, C. M., Lord, B. I., Brotherton,

D., Christison, R., Craig, S., Cribbes, S., Edwards, R. M., Evans, S. J., Gilbert, R., Morgan, P., Randle, E., Schofield, N., Varley, P. G., Fisher, J., Waltho, J. P., and Hunter, M. G. (1999) *J. Biol. Chem.* **274,** 16077–16084
54. Kuloğlu, E. S., McCaslin, D. R., Markley, J. L., and Volkman, B. F. (2002) *J. Biol. Chem.* **277,** 17863–17870
55. Hartley, O., and Offord, R. E. (2005) *Curr. Protein Pept. Sci.* **6,** 207–219
56. Loetscher, P., and Clark-Lewis, I. (2001) *J. Leukoc. Biol.* **69,** 881–884
57. Handel, T. M., Johnson, Z., Rodrigues, D. H., dos Santos, A. C., Cirillo, R., Muzio, V., Riva, S., Mack, M., Deruaz, M., Borlat, F., Vitte, P. A., Wells, T. N., Teixeira, M. M., and Proudfoot, A. E. (2008) *J. Leukoc. Biol.* **84,** 1101–1108
58. Shahrara, S., Proudfoot, A. E., Park, C. C., Volin, M. V., Haines, G. K., Woods, J. M., Aikens, C. H., Handel, T. M., and Pope, R. M. (2008) *J. Immunol.* **180,** 3447–3456
59. Ali, S., O'Boyle, G., Mellor, P., and Kirby, J. A. (2007) *Mol. Immunol.* **44,** 1477–1482
60. O'Boyle, G., Mellor, P., Kirby, J. A., and Ali, S. (2009) *FASEB J.* **23,** 3906–3916
61. Wijtmans, M., Verzijl, D., Leurs, R., de Esch, I. J., and Smit, M. J. (2008) *Chem. Med. Chem.* **3,** 861–872
62. Jansma, A. L., Kirkpatrick, J. P., Hsu, A. R., Handel, T. M., and Nietlispach, D. (2010) *J. Biol. Chem.* **285,** 14424–14437